Received June 2001
Accepted May 2002

Effect of viscosity ratio, spin and Reynolds number on the flow characteristics about a liquid sphere in a gas stream

M.A. Antar and M.A.I. El-Shaarawi
Department of Mechanical Engineering, King Fahd University of Petroleum and Minerals, Dhahran, Saudi Arabia

Keywords *Boundary layers, Numerical methods, Flow*

Abstract *Boundary-layer flow around a spinning liquid sphere moving steadily in a gas stream is investigated numerically. The shear stress exerted on the sphere's surface results in surface rotation in the meridional direction in addition to the azimuthal velocity resulting from the spinning of the liquid sphere. The parameters controlling the flow around the sphere are the external flow Reynolds number (Re), the liquid-to-gas viscosity ratio (μ^*) and the spinning parameter $(Re_r/Re)^2$. The effect of these parameters on the velocity components (namely the meridional, radial and azimuthal velocity components) and on the shear stress is shown. Moreover, their effect on the location of external flow point of separation is also demonstrated.*

Nomenclature

a = Sphere radius
r = Radius of a circular cross-section of the spherical droplet by a plane perpendicular to the main gas stream direction
R = Dimensionless value of r, $2r/(a\,\mathrm{Re})$
Re = Reynolds number, $2U_\infty a/\nu$
Re_r = Rotational Reynolds number, $2\Omega a^2/\nu$
t_x = Shear stress in the meridional direction on the spherical droplet's surface, $\mu(\partial u/\partial z)_0$
t_y = Shear stress in the azimuthal direction on the spherical droplet's surface, $\mu(\partial v/\partial z)_0$
T_x = Dimensionless shear stress in the meridional direction, $t_x(\sqrt{\mathrm{Re}/2})/(\rho U_\infty^2)$
T_y = Dimensionless shear stress in the azimuthal direction, $t_y(\sqrt{\mathrm{Re}/2})/(\rho U_\infty^2)$
u = Meridional (x-direction) component of velocity
U = Dimensionless meridional component of velocity, u/U_∞
u^* = Velocity component in the x-direction for the potential flow outside the external boundary layer, $-(\partial\psi/\partial r)/(r\sin\theta) = U_\infty \sin\theta[1 + a^3/(2r^3)]$
U^* = Dimensionless potential velocity component in the x-direction for external flow, u^*/U_∞
U_∞ = Free stream velocity in the exterior flow
v = Azimuthal velocity component
v_0 = Circumferential velocity at a point on the spherical droplet surface, Ωr
V = Dimensionless azimuthal velocity component at any point, $v/\Omega a$
V_0 = Dimensionless azimuthal velocity

International Journal of Numerical Methods for Heat & Fluid Flow, Vol. 12 No. 7, 2002, pp. 800-816 .

DOI 10.1108/09615530210443034

The authors acknowledge King Fahd University of Petroleum and Minerals for supporting this work under the Fast Track Project # FT2000-23.

component at a point on the droplet surface, r/a

w = Radial (z-direction) velocity component

w^* = Radial (z-direction) velocity component for potential flow outside the external boundary layer, $(\partial\psi/\partial\theta)/(r^2 \sin\theta) = -U_\infty \cos\theta[1 - a^3/r^3]$

W = Dimensionless radial velocity component, w/U_∞

W^* = Dimensionless radial velocity component for the external potential flow, w^*/U_∞

x = Meridional distance (along the circular generator of the droplet's spherical surface) measured from the stagnation point

X = Dimensionless meridional distance along the surface measured from the stagnation point, $2x/\mathrm{Re}\ a$

z = Distance from the droplet's spherical surface measured along the normal to the surface in the radial direction, being positive for the external flow and negative inside the sphere

Z = Dimensionless distance perpendicular to the surface in the radial direction, z/a

Greek symbols

θ = Center angle measured from the frontal stagnation line

μ = Dynamic fluid viscosity

μ^* = Interior-to-exterior (liquid-to-gas) dynamic viscosity ratio, μ_l/μ_g

ν = Kinematic viscosity of the fluid

Ω = Angular velocity of the sphere

ψ = Stream function of external potential flow far away from the droplet, given by $\psi = 0.5\, u_\infty\, r^2 \sin^2\theta(1 - a^3/r^3)$

Subscripts

g = Gas phase

l = Inside the liquid sphere (droplet)

o = On the sphere surface

s = At separation point for fluid flow

Introduction

This work deals with the problem of flow around a spinning liquid sphere subjected to a uniform stream in the direction of its axis of spin. The sphere also experiences a shear stress on its outer surface that results in the rotation of this surface in the meridional direction leading to three-dimensional governing equations that are solved numerically. Practical applications of this analysis can be found in the case of a fuel droplet injected with swirl into a combustion chamber and in the case of a water droplet in spray-irrigation or fire fighting with swirl (if any).

Schlichting (1953) used a momentum integral technique and Hoskins (1954) reported that the separation point of the laminar boundary layer is advanced at the rear hemisphere due to the solid sphere rotation. The three-dimensional flow around a spinning body of revolution was analyzed by Parr (1964) using the boundary-layer theory. El-Shaarawi *et al.* (1985) investigated the boundary-layer flow about a spinning solid sphere for high values of Reynolds number and spin parameter. They also reported that increasing the spin parameter $(\mathrm{Re}_r/\mathrm{Re})^2$ shifts the point of laminar flow separation forward. Rao and Sekhar (1993) analyzed numerically the axisymmetric rotating flow around a spinning solid sphere at small Reynolds numbers such that the diameter about which the sphere spins lies along the axis of the rotating fluid. They solved the complete Navier-Stokes equations in the stream function-vorticity format. Schmitt (1997) analyzed the viscous flow around a sphere spinning at a constant angular velocity for large Reynolds numbers.

The unsteady boundary-layer flow past an impulsively started translating and spinning rotational symmetric body was studied by Ece (1992), where the stream function and the velocity swirl component were expanded in series in powers of time. He reported that the sphere rotation reduces the drag and the separation angle. Ferriera *et al.* (1998) studied analytically the transient motion of a dense rigid sphere falling in light liquid. They obtained closed form solutions of instantaneous position, velocity and acceleration of the sphere. Kalro and Tezduvar (1998) used finite-element method to also investigate the three-dimensional unsteady flow past a sphere.

Raghavarao and Pramadavalli (1989a, b) studied the flow of steady incompressible fluid rotating with a constant angular velocity and moving past a sphere for small values of Reynolds number where the Navier-Stokes equations were linearized using the Oseen approximation. They concluded that the rotation decreased the values of the stream function. Then, they solved the non-linear Navier-Stokes equations numerically in the stream function-vorticity form and compared the results of the two models. The unsteady flow past a sphere was investigated numerically for oscillatory and accelerated motion, respectively, by Chang and Maxey (1994, 1995) at low to moderate Reynolds numbers.

El-Shaarawi *et al.* (1997) considered the flow about and inside a non-spinning liquid sphere moving steadily in another immiscible fluid, boundary-layer equations were used to investigate the flow field for large Reynolds number and for a wide range of interior-to-exterior viscosity ratio. The shear stress on the fluid-sphere-surface induces internal motion inside the sphere that can be represented by the well-known Hill's vortex. However, the strength of the vortex is reduced because of the boundary layer in the liquid phase.

To the best of the authors' knowledge, no previous work investigated the three-dimensional flow field around a spinning liquid sphere at moderate to high Reynolds numbers. This work aims at covering the still-existing gap in the literature by analyzing the hydrodynamics of a spinning liquid sphere in a gas stream. The effect of the flow parameters on the velocity profiles, the shear stress and the angle of flow separation will be presented.

Governing equations and boundary conditions

Figure 1a depicts the problem under consideration and the coordinate system. The flow field is assumed to be axisymmetric ($\partial/\partial\vartheta = 0$) and both the fluids have constant properties. Reynolds number is assumed large enough for the boundary-layer model to be applied ($\mathrm{Re} \gg 1$). Weber number is assumed small enough so that the drop remains spherical in shape ($\mathrm{We} \ll 1$). The effects of gravity, chemical reaction, compressibility, phase change and surface active impurities are absent. Under these assumptions, the non-dimensional continuity and momentum equations are:

Mass conservation

$$\frac{\partial U}{\partial X}+\frac{\mathrm{Re}}{2}\frac{\partial W}{\partial Z}+\frac{U}{R}\frac{\mathrm{d}R}{\mathrm{d}X}+\mathrm{Re}\frac{W}{1+Z}=0 \tag{1}$$

Momentum conservation in meridional direction

$$U\frac{\partial U}{\partial X}+\frac{\mathrm{Re}W}{2}\frac{\partial U}{\partial Z}-\left(\frac{\mathrm{Re}_r}{\mathrm{Re}}\right)^2\frac{V^2}{R}\frac{\mathrm{d}R}{\mathrm{d}X}=U^*\frac{\partial U^*}{\partial X}+\frac{\partial^2 U}{\partial Z^2} \tag{2}$$

Momentum equation in azimuthal direction

$$U\frac{\partial V}{\partial X}+\frac{UV}{R}\frac{\partial R}{\partial X}+\frac{\mathrm{Re}}{2}W\frac{\mathrm{d}V}{\mathrm{d}Z}=\frac{\partial^2 V}{\partial Z^2} \tag{3}$$

The above equations are subject to the following boundary conditions

$$\left.\begin{aligned}
&\text{for } Z=0,\ X=0; \quad U=V=W=0\\
&\text{for } Z=\infty,\ X\geq 0 \text{ (far away from the droplet)}; \quad U=U^*,\ V=0\\
&\text{for } Z>0 \text{ and } X=0, \text{ and } W=W^*,\ U=V=0\\
&\text{for } Z=0,\ X>0 \text{ (droplet surface)}; \quad U=U_1,\\
&\qquad\qquad \frac{\partial U}{\partial Z}=-\mu^*\frac{\partial U_1}{\partial Z_1} \text{ (shear stress equality)},\\
&\qquad\qquad W=0 \text{ and } V=(\mathrm{Re}/2)\ R
\end{aligned}\right\} \tag{4}$$

Numerical method of solution

The numerical grid is shown in Figure 1b. A typical mesh point (i,j) designates the progress in the radial direction (i) and meridional direction (j), where $i=1$ represents the surface of the sphere and increases radially till the edge of the boundary layer, while $j=1$ represents the front stagnation line and increases till the point of external flow separation is encountered and the solution is stopped. The governing equations (1-3) along with the boundary conditions (4) can be written in finite-difference forms as follows:

$$\begin{aligned}
&\frac{U_{i+1,j+1}+U_{i,j+1}-U_{i+1,j}-U_{i,j}}{2\Delta X_{i+1/2}}+\frac{\mathrm{Re}}{2}\frac{W_{i+1,j+1}-W_{i,j+1}}{\Delta Z}\\
&+\frac{\mathrm{Re}(W_{i+1,j+1}+W_{i,j+1})}{2(1+Z_{i+1/2})}+\frac{(U_{i+1,j+1}+U_{i,j+1})\mathrm{Re}\ \cot(j\Delta\theta)}{4(1+Z_{i+1/2})}=0
\end{aligned} \tag{5}$$

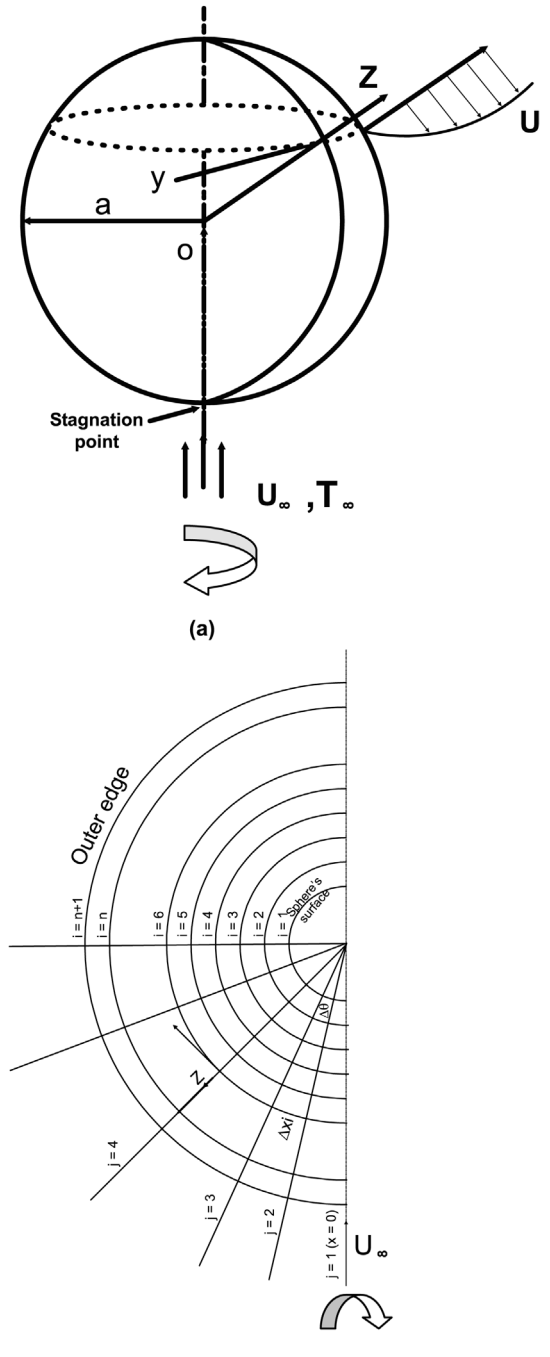

Figure 1.
(a) Coordinate system,
(b) numerical grid

$$U_{i,j}\frac{U_{i,j+1}-U_{i,j}}{\Delta X_i}+\frac{\mathrm{Re}}{2}W_{i,j}\frac{U_{i+1,j+1}-U_{i-1,j+1}}{2\Delta Z}$$
$$-\left(\frac{\mathrm{Re}_r}{\mathrm{Re}}\right)^2\frac{V_{i,j}V_{i,j+1}}{2[1+(i-1)\Delta Z]}\cot(j\Delta\theta)$$
$$=\frac{9}{8}\sin(j.\Delta\theta).\mathrm{Re}\ \cos(j.\Delta\theta)+\frac{U_{i+1,j+1}-2U_{i,j+1}+U_{i-1,j+1}}{\Delta Z^2} \quad (6)$$

$$U_{i,j}\frac{V_{i,j+1}-V_{i,j}}{\Delta X_i}+\frac{\mathrm{Re}}{4}U_{i,j}\frac{V_{i,j+1}-V_{i,j}}{1+(i-1)\Delta Z}\cot\left(j-\frac{1}{2}\right)\Delta\theta$$
$$+W_{i,j}\frac{V_{i+1,j+1}+V_{i+1,j}-V_{i-1,j}-V_{i-1,j+1}}{4\Delta Z}\frac{\mathrm{Re}}{2}$$
$$=\frac{V_{i+1,j+1}+V_{i+1,j}-2V_{i,j+1}-2V_{i,j}+V_{i-1,j+1}+V_{i-1,j}}{2(\Delta Z^2)} \quad (7)$$

and the boundary conditions are

$$\text{for } j=1 \text{ and } i\geq 1: U_{i,1}=V_{i,1}=0,\quad W_{i,1}=-1+\frac{1}{[1+(i-1)\Delta Z]^3}$$
$$\text{for } i=n+1 \text{ and } j>1: U_{n+1,j}=\left[1+\frac{1}{2(1+n\Delta Z)^3}\right]$$
$$\sin[(j-1)\Delta\theta]V_{n+1,j}=0 \quad (8)$$
$$\text{for } i=1 \text{ and } j>1: U_{1,j}=\mathrm{U}_{il,j},\quad W_{1,j}=W_{l1,j}=0,$$
$$\frac{U_{2,j}-U_{1,j}}{\Delta Z}=\frac{\mu^*}{\Delta Z_1}(U_{l2,j}-U_{l1,j})$$

It is noted that in the given finite-difference equations, the variables with subscript $j+1$ indicate unknown values, while the variables with subscript j are known values. Moreover, the equations are linearized by assuming that where the product of two unknowns occurs, one of them is given by its value from the previous meridional step. On specifying the values of Re, μ^* and $(\mathrm{Re}_r/\mathrm{Re})^2$, equation (7) is solved for the second meridional step ($j=2$, $i=1,2,\ldots,\ n-1$) using Thomas method for the obtained $(n-1)$ simultaneous equations. Having calculated the values of V at the second meridional step, these values are used to solve equation (6) for the meridional velocity values (U) using the same method to similarly solve the obtained (n) equations. It is worth mentioning that the surface velocity $U_{0,2}$ is greater than zero because of the shear stress effect on the sphere's surface that results in the

surface rotation. The condition on the surface is unknown and can be obtained from the solution of the pertinent matrix after using the following equation to determine $U_{l2,j}$ without the need to solve furthermore inside the sphere.

$$U_{l2,j} = \frac{U_{2,j}}{\mu^*} - U_{1,j}\left(\frac{1}{\mu^*} - 1\right)$$

This equation is obtained by applying the continuity of the shear stress in both the gas and liquid phases and considering $\Delta Z = \Delta Z_1$. Using the computed values of V and U in the second meridional step, equation (5) can be solved for W in a step-by-step manner. Then the solution is advanced to the next meridional step and the whole procedure is repeated till the point of external flow separation, which is characterized by the condition $\partial U/\partial Z = 0$, is reached.

The selection of n is done as follows. An initial value of 20 is assumed and then on solving for the meridional velocity component, the value at the uppermost point is compared with the potential flow velocity component at the same meridional station. If they are close in tangent, the solution is advanced to the next meridional station, otherwise the value of n is increased by 2 and the solution is repeated for the same meridional station and the computed values of U are accepted, if the same criteria is satisfied. When the point of separation is reached, the solution is stepped back to the previous meridional station and the increment $\Delta\theta$ is changed from 1 to 0.1° in order to accurately estimate the separation point. The code has the advantage of being fast and requires low computer storage capacity.

The truncation error due to the finite-difference approximation of equations (1-3) is proportional to ΔX and ΔZ^2 and it vanishes as the mesh size tends to zero confirming the consistency of the finite-difference equations (5-7) with their original partial differential equations (1-3). In addition, the finite-difference equations are found to be stable for all mesh sizes as long as the down-stream meridional velocity is positive (i.e. before the point of external flow separation).

Results and discussion

Three parameters control the flow around the liquid sphere. These parameters are: Reynolds number Re, the dynamic viscosity ratio μ^*, and the spinning parameter $(\mathrm{Re}_r/\mathrm{Re})^2$. It is worth mentioning that inspite of the fact that the computer code can cope with large values of the controlling parameters, the value of Reynolds number is limited to 125 to keep the Weber number small enough to avoid droplet deformation.

For example, a simple calculation for a liquid hydrocarbon droplet moving in air of a temperature of about 500°C at U_∞ about 1 m/s gives $\mu_{\mathrm{gas}}\, U_\infty/\sigma \sim$ O (10^{-3}). Since $\mathrm{We} = \mu_{\mathrm{gas}}\, U_\infty \mathrm{Re}/\sigma$, then the previous example gives $\mathrm{We} \sim \mathrm{O}(10^{-1})$ which is $\ll 1$. In this study, the spin parameter $(\mathrm{Re}_r/\mathrm{Re})^2$, which

represents the ratio between centrifugal force and inertial force, ranges from 0 to 500 and the viscosity ratio ranges from 1.01 to 5. Results are obtained to show the effect of these parameters on the three velocity components within the boundary layer, the shear stress and the point of external flow separation.

Figure 2a shows the meridional velocity profile at different meridional stations for a Reynolds number of 100, a liquid-to-gas viscosity ratio (μ*) of 1.5, and $(\mathrm{Re}_r/\mathrm{Re})^2 = 0$. It is clear from this figure that the hydrodynamic boundary layer thickness increases as the meridional angle θ increases. Figure 2b shows the effect of the spin on the meridional velocity distribution. The spin ($(\mathrm{Re}_r/\mathrm{Re})^2 > 0$) results in fluid acceleration within the boundary layer due to the centrifugal force acting on the fluid layers close to the spherical droplet surface. This effect is absent in the non-spinning sphere, i.e. for $(\mathrm{Re}_r/\mathrm{Re})^2 = 0$ (Figure 2a). Moreover, it is not clear for low values of $(\mathrm{Re}_r/\mathrm{Re})^2$ and starts to appear as $(\mathrm{Re}_r/\mathrm{Re})^2$ increases and is shown clearly in Figure 3a for various values of the spin parameter $(\mathrm{Re}_r/\mathrm{Re})^2$. It can also be noticed that the meridional velocity at the sphere surface is not equal to zero as in the case of flow about a solid sphere because of the rotation of the sphere's surface due to the shear stress exerted by the external flow. Figure 3b shows other meridional velocity distribution but with viscosity ratio $\mu^* = 1.05$, higher surface velocities can be noticed for this low viscosity ratio.

Figure 4 depicts the azimuthal velocity profiles around the sphere where the velocity V has a certain value equation (4) at the surface of the sphere and this value reduces to zero in the undisturbed flow region far away from the surface, outside the azimuthal velocity boundary layer. The thickness of this boundary layer increases as the meridional angle θ increases due to the tangential momentum diffusion within such an azimuthal velocity boundary layer. Increasing the spin parameter increases the azimuthal surface velocity and consequently leads to thinner boundary layers as shown in Figure 5.

The effect of the spin parameter on the radial velocity profiles is shown in Figure 6a at different meridional angles for $\mathrm{Re} = 100$, a viscosity ratio $\mu^* = 1.5$ and two values of $(\mathrm{Re}_r/\mathrm{Re})^2$. The profiles are negative for meridional angles <90 while they are positive for meridional angles ≥ 90. This behavior shows that the radial velocity component transports the boundary-layer fluid towards the sphere surface (negative values of W) in the accelerated region of the flow ($\theta < 90$) compared with the radial velocity profiles in the adverse region ($\theta > 90°$), where the tendency changes to delivery of the fluid away from the sphere. The effect of Reynolds number on the radial velocity profiles for two selected meridional angles is shown in Figure 6b. Increasing the Reynolds number always has the effect of decreasing the boundary-layer thickness in the accelerating region and hence decreases the values of W for a given Z, thus delaying the point of flow separation.

Figure 7a shows the distribution of the dimensionless meridional wall shear stress at the surface of the sphere (T_x) for three selected values of the Reynolds

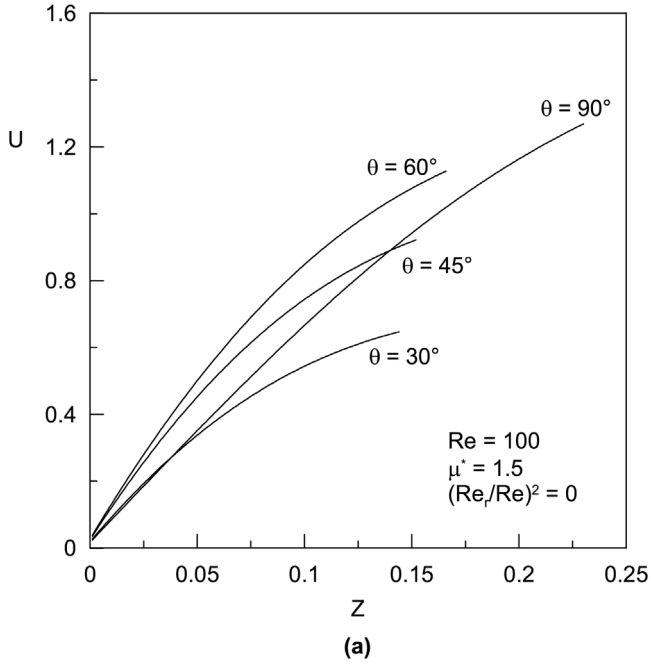

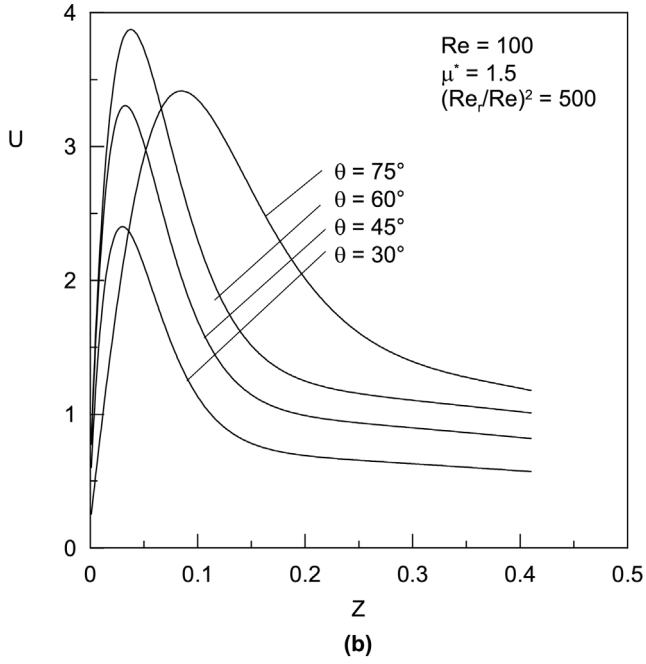

Figure 2.
(a) Meridional velocity profiles at different angles for a non-spinning liquid sphere,
(b) meridional velocity profiles at different angles for a spinning liquid sphere

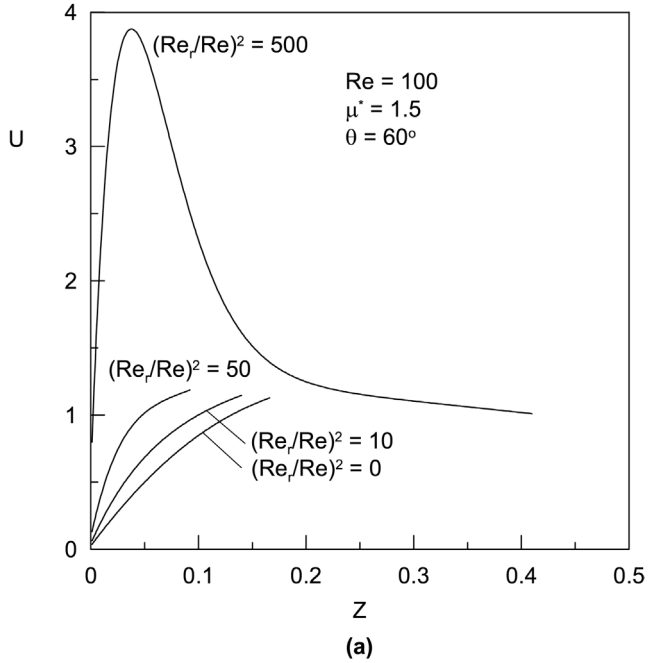

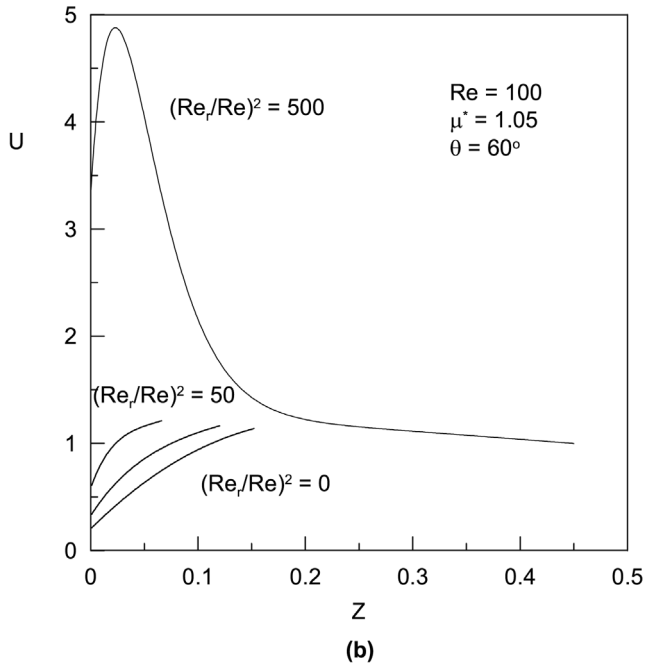

Figure 3.
(a) Effect of the spin parameter on the meridional velocity profile at a given meridional location, $\mu^* = 1.5$, Re = 100, $\theta = 60°$, (b) effect of the spin parameter on the meridional velocity profile at a given meridional location, $\mu^* = 1.01$, Re = 100, $\theta = 45°$

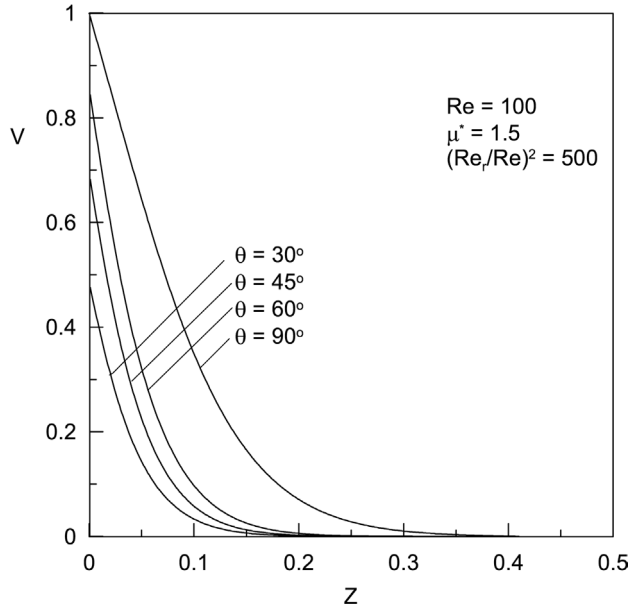

Figure 4.
Azimuthal velocity profile for different angles

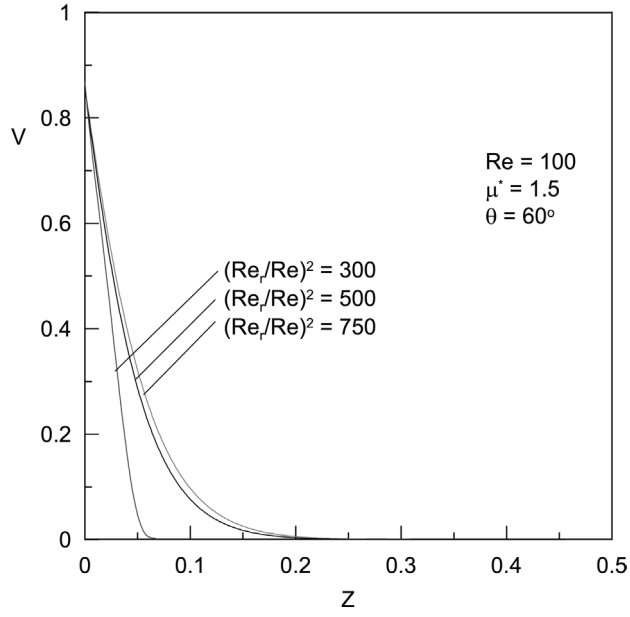

Figure 5.
Effect of the spin parameter on the azimuthal velocity profile

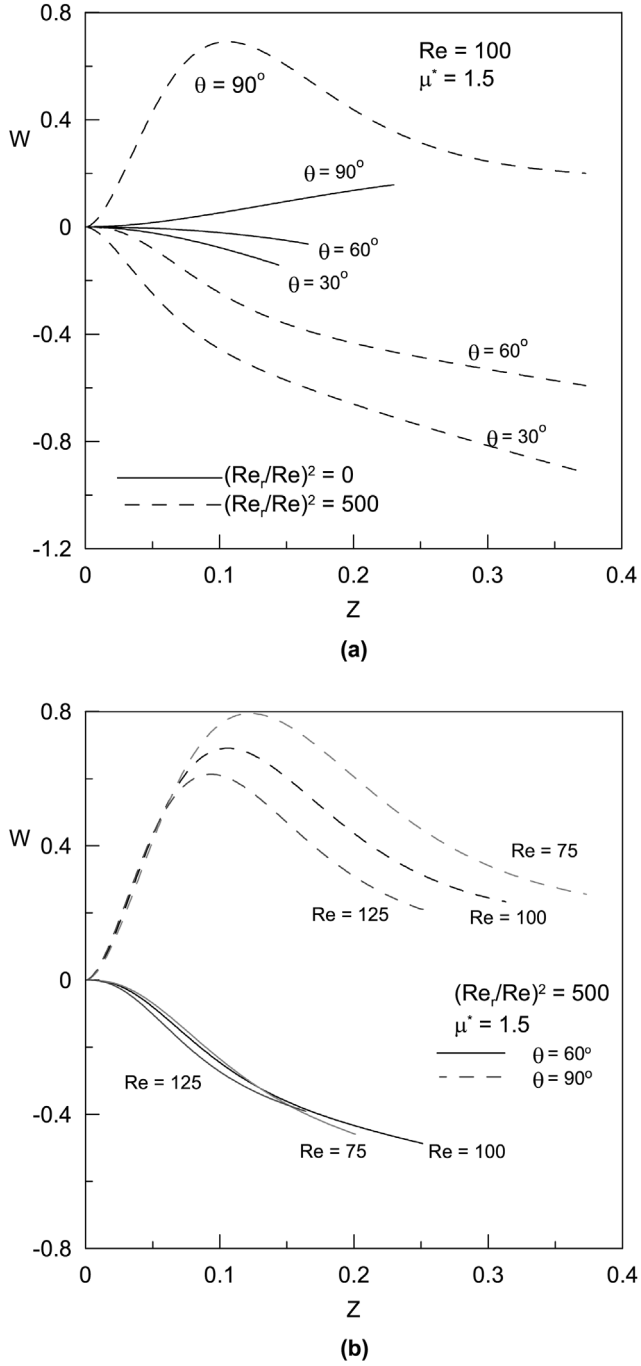

Figure 6.
(a) Radial velocity profiles at different angles for two values of the spin parameter, (b) radial velocity profiles at two different angles for three values of Reynolds number

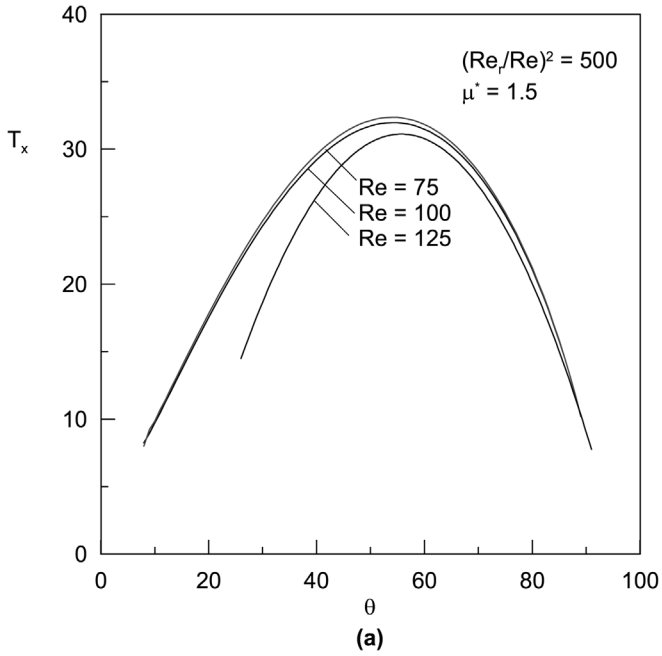

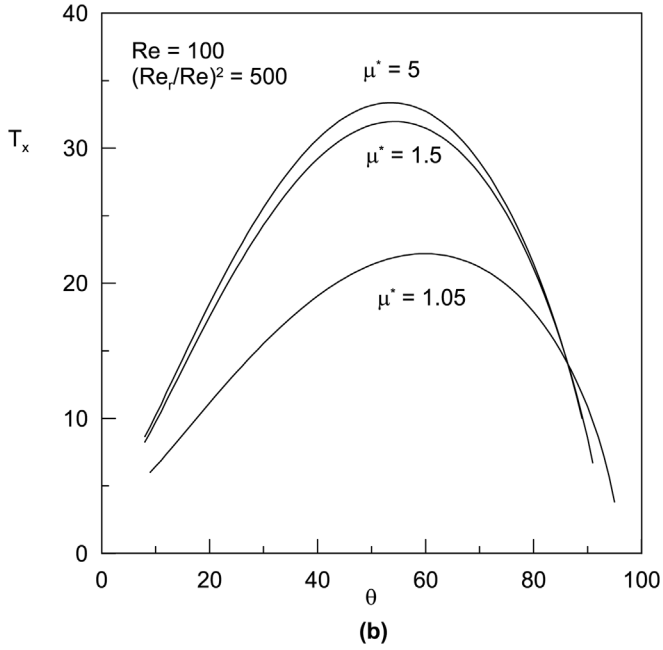

Figure 7.
(a) Effect of Re on the meridional shear stress; (b) effect of viscosity ratio on the meridional shear stress; (c) effect of the spin parameter on the meridional shear stress; and (d) effect of the spin parameter on the azimuthal shear stress

(Continued)

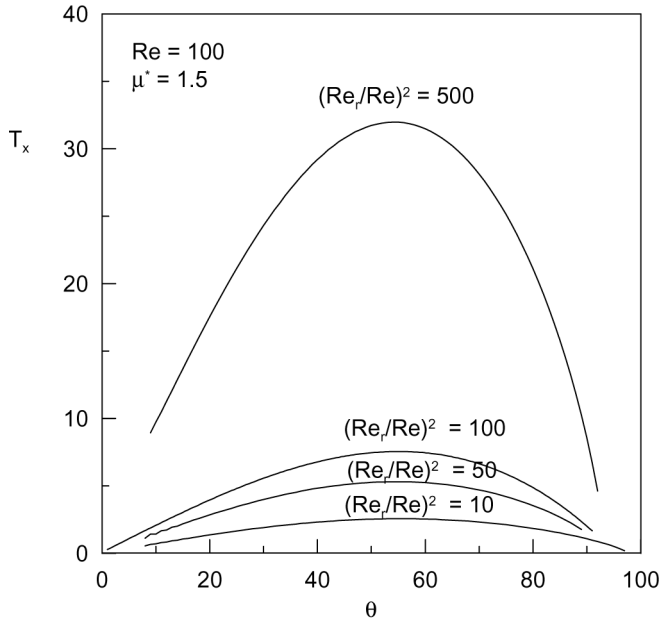
Re = 100
μ* = 1.5
(Re_r/Re)² = 500
(Re_r/Re)² = 100
(Re_r/Re)² = 50
(Re_r/Re)² = 10
T_x
θ
0
10
20
30
40
0
20
40
60
80
100

(c)

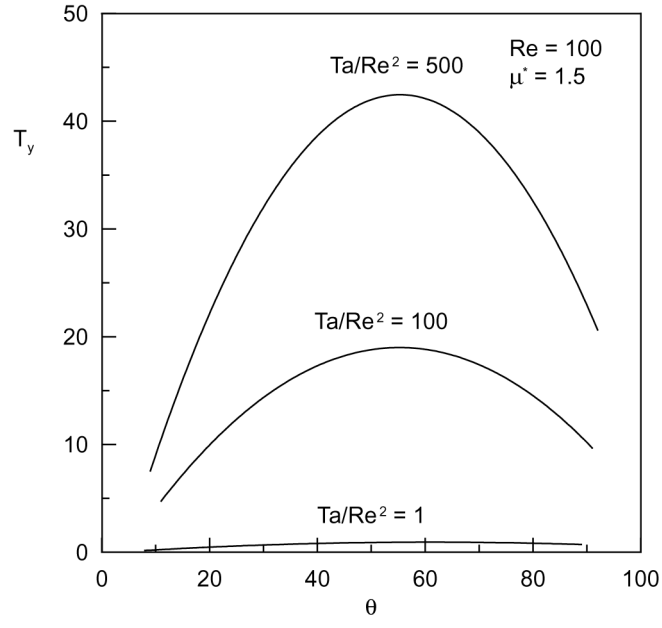
Ta/Re² = 500
Re = 100
μ* = 1.5
Ta/Re² = 100
Ta/Re² = 1
T_y
θ
0
10
20
30
40
50
0
20
40
60
80
100

(d)

Figure 7.

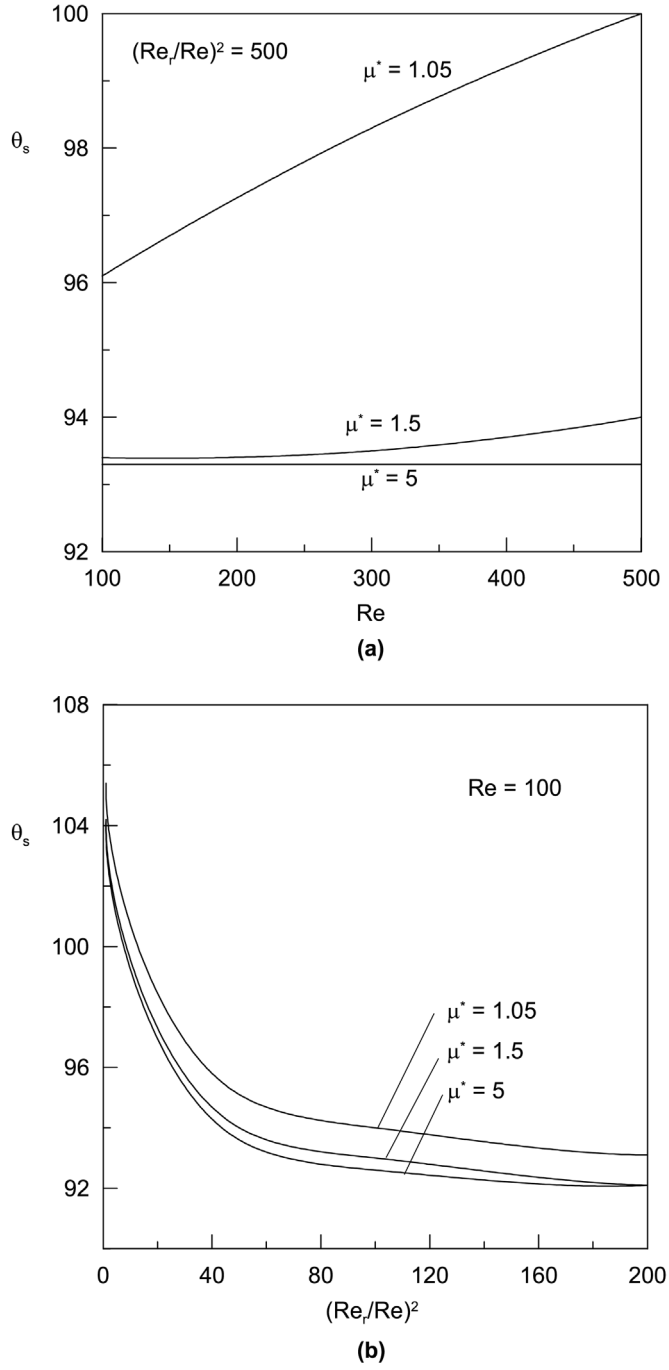

Figure 8.
Effect of the spin parameter on the angle of separation

number (Re = 75, 100 and 125), for given values of the viscosity ratio ($\mu^* = 1.5$) and the spin parameter ($(Re_r/Re)^2 = 500$). The meridional shear stress generally increases with the meridional angle, reaches a maximum value at a meridional angle of about 60° and then it decreases until the point of external flow separation is reached. Increasing the Reynolds number results in an increase in the surface velocity and hence reduces the meridional shear stress. The effect of the viscosity ratio on the shear stress is shown in Figure 7b where decreasing the viscosity ratio would have a similar effect as increasing the Reynolds number, i.e. the shear stress decreases due to the increased surface velocity. Figure 7c shows the effect of the spin parameter $(Re_r/Re)^2$ on the meridional shear stress. The increase in the values of the meridional shear stress with $(Re_r/Re)^2$ is due to the fluid acceleration within the boundary layer at higher values of the spin parameter. Figure 7d shows the effect of the spin parameter $(Re_r/Re)^2$ on the dimensionless azimuthal shear stress (T_y). Increasing the spin parameter leads to increasing the velocity gradient within the hydrodynamic boundary layer and hence to higher values of the azimuthal shear stress.

The effect of $(Re_r/Re)^2$ on the angle of flow separation is shown in Figure 8 where increasing the spin parameter results in retarded angles of external flow separation. This can be explained with the aid of Figure 2b which indicates thinner boundary layers corresponding to higher values of the spin parameter. On the other hand, Figure 8 shows that the angle of external flow separation decreases with μ^*. This is because the higher the values of μ^* the less viscous the external fluid and hence the smaller the velocities within the external boundary layer for a given Re.

Conclusions

In this study, the three velocity components around a liquid sphere moving steadily in a gas stream fluid and spinning with a constant angular velocity have been presented. The main parameters affecting the flow field are the external flow Reynolds number, the interior-to-exterior viscosity ratio and the spin parameter $(Re_r/Re)^2$. Increasing the Reynolds number or decreasing the viscosity ratio has an effect of increasing the meridional velocity within the boundary layer and delaying the point of external flow separation. On the other hand, increasing the spin parameter $(Re_r/Re)^2$ results in accelerated flow within the boundary layer and hence thinner boundary layers and retarded separation points.

References

Chang, E.J. and Maxey, M.R. (1994), "Unsteady flow about a sphere at low to moderate Reynolds number; oscillatory motion", *J. Fluid Mechanics*, Vol. 277, pp. 347-79.

Chang, E.J. and Maxey, M.R. (1995), "Unsteady flow about a sphere at low to moderate Reynolds number. Part 2. Accelerated motion", *J. Fluid Mechanics*, Vol. 303, pp. 133-53.

Ece, Mehmet C. (1992), "Initial boundary layer flow past a translating and spinning rotational symmetric body", *J. Engineering Mathematics*, Vol. 26 No. 3, pp. 415-28.

El-Shaarawi, M.A.I., El-Refai, M.F. and El-Bedeawi, S.A. (1985), "Numerical solution of boundary layer flow about a rotating sphere in an axial stream", *J. Fluids Engineering*, Vol. 107, pp. 97-104.

El-Shaarawi, M.A.I., Al-Farayedhi, A.A. and Antar, M.A. (1997), "Boundary layer flow about and inside a liquid sphere", *ASME J. Fluids Engineering*, Vol. 119, pp. 42-9.

Ferreira, J.M., Duarte Naia, M. and Chabra, R.P. (1998), "Analytical study of the transient motion of a dense rigid sphere in an incompressible Newtonian fluid", *Chemical Engineering Communications*, Vol. 168, pp. 45-58.

Hoskins, N.E. (1954), "The laminar boundary layer on a rotating sphere", in *Fifty Years of Boundary Layer Research*, Braunschweig, pp. 127-31.

Karlo, V. and Tezduvar, T. (1998), "3D computation of unsteady flow past a sphere with a parallel finite element method", *Computer Methods in Applied Mechanics and Engineering*, Vol. 151, pp. 267-76.

Parr, O. (1964), "Flow in the three dimensional boundary layer on a spinning body of revolution", *AIAA J.*, Vol. 2 No. 2, pp. 361-3.

Raghavarao, C.V. and Pramadavalli, K. (1989a), "Numerical studies of slow viscous rotating flow past a sphere. II", *Int. J. Numerical Methods in Fluids*, Vol. 9 No. 11, pp. 1307-19.

Raghavarao, C.V. and Pramadavalli, K. (1989b), "Numerical studies of slow viscous rotating flow past a sphere. III", *Int. J. Numerical Methods in Fluids*, Vol. 9 No. 11, pp. 1321-9.

Rao, C.V.R. and Sekhar, T.V.S. (1993), "Flow past a spinning sphere in a slowly rotating fluid at small Reynolds numbers-A numerical study", *Int. J. Engineering Science*, Vol. 31 No. 9, pp. 1219-31.

Schlichting, H. (1953), "Laminar flow about a body of revolution in an axial stream", *NACA TM*1415

Schmitt, H. (1997), "Flow around a spinning sphere at large Reynolds numbers flow", *Advances in Fluid Mechanics*, Vol. 11, pp. 75-87.